Field Experiments with Doppler Compensation in High-Frequency Underwater Acoustic Communication System

Deniz Unal, Kerem Enhos, Emrecan Demirors and Tommaso Melodia

Institute for The Wireless Internet of Things, Northeastern University, Boston, MA, USA

Email: {unal.d, enhos.k, e.demirors, melodia}@northeastern.edu

Abstract—Underwater acoustic communication and networking have been instrumental in enabling various commercial and military applications such as underwater surveillance, environmental monitoring, data-driven intelligent aquaculture, and unmanned underwater vehicles. However, the development of an underwater communication and networking system poses significant challenges due to spatially and temporally varying underwater acoustic channels. These channels are subject to severe multipath propagation and the Doppler effect, which can impose frequency-dependent distortions on underwater acoustic signals through frequency shifts and spreading. In high-frequency underwater acoustic communication systems, the Doppler effect is amplified, making its estimation and compensation even more challenging. In this paper, we present a detailed set of field experiments characterizing the Doppler effect in a high-frequency underwater acoustic channel. We also introduce a multicarrier communication system incorporating a Doppler estimation and compensation method. Through extensive field experiments, we quantify the performance of the Doppler estimation and compensation technique over high-frequency channels.

Index Terms—Underwater Wireless Communication, Software-Defined Modem, wideband channels, Doppler Effect

I. INTRODUCTION

Underwater acoustic communication and networking has already been an enabling technology for many commercial and military applications. Among these are underwater surveillance, environmental monitoring, data-driven intelligent aquaculture, and unmanned underwater vehicles. However, developing an underwater communication and networking system is not a trivial task. Spatially and temporally varying underwater acoustic channels possess formidable challenges, including severe multipath propagation and the Doppler effect. In particular, the Doppler effect is much more pronounced in underwater acoustic channels, compared to radio frequency channels, due to the relatively low speed of sound in water ($\sim 1500\,\mathrm{m/s}$) and inherently wideband channels with a small ratio of carrier frequencies and channel bandwidths [1], [2].

The Doppler effect is mainly caused by the relative motion between the transmitter and receiver. It is an inherent problem for network nodes on mobile platforms such as underwater

vehicles (e.g., unmanned underwater vehicles (UUVs)). On the other hand, static underwater nodes, which are typically anchored, also experience unintentional motion due to surface tides and currents. In addition to node mobility, surface waves, and currents can also affect propagation speed and paths translated as relative motion between transmitter and receiver node pairs.

Overall, the Doppler effect can impose severe frequency-dependent distortions in the form of frequency shifts and spreading to underwater acoustic signals, which, without compensation, can cause substantial performance degradation. Especially in multicarrier communication methods, which have prevailed in recent underwater systems thanks to their decent performance with low complexity in high dispersive channels [3], [4], the performance degradation due to the Doppler effect is amplified. The frequency-dependent Doppler shifts and spreading would impose substantial inter-carrier interference (ICI) and cause subcarriers to be no longer orthogonal.
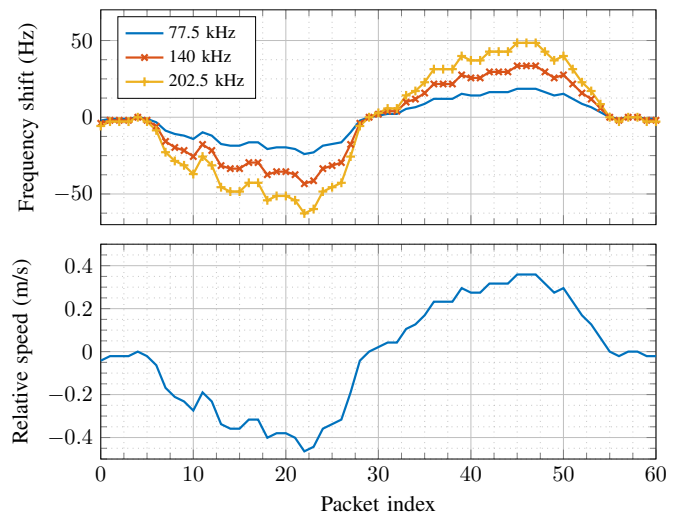

Fig. 1: Mobility-induced frequency shifts of different subcarriers in a high-frequency ZP-OFDM system

Doppler estimation and compensation techniques have received a lot of interest from the research community over the last few decades [3], [5]–[8]. Prior work on Doppler estimation and compensation has mostly focused on systems

with relatively low carrier frequencies ($< 100\,\text{kHz}$) and narrow bandwidths ($<10\,\text{kHz}$). However, with the requirement of higher data rate communication links, using larger frequency bands and higher carrier frequencies is becoming a necessity. Effective Doppler estimation and compensation in high-frequency systems is particularly challenging due to the frequency-dependent nature of the Doppler effect. To give a practical example, we have investigated the mobility-induced Doppler effect on different subcarriers of a multicarrier communication system (i.e., zero-padded (ZP)-OFDM). The system was using 8192 subcarriers allocated over a total bandwidth of $< 125\,\text{kHz}$ and centered at $< 140\,\text{kHz}$. Figure 1 shows how mobility introduces varying frequency shifts to different subcarrier bands. More specifically, a relative speed of approximately only $0.4\,\text{m/s}$ causes a frequency shift of $15\,\text{Hz}$ to a subcarrier centered at $77.5\,\text{kHz}$ while it causes a $40\,\text{Hz}$ shift to another subcarrier located at $202.5\,\text{kHz}$. This means that higher frequencies subcarriers can experience frequency shifts 3 to 4 times of a single subcarrier size ($15.25\,\text{Hz}$).

This case study clearly shows that Doppler estimation and compensation could be an even more challenging problem for high-frequency underwater acoustic communication systems. Therefore, in this paper, we present a detailed set of field experiments characterizing the Doppler effect in a high-frequency underwater acoustic channel. Moreover, we present a multicarrier communication system incorporating a Doppler estimation and compensation method. Through extensive field experiments, we quantify the performance of the used Doppler estimation and compensation technique over high-frequency channels. The rest of this paper is organized as follows. Section II describes the packet design and Doppler estimation and compensation method. Section IV describes the testbed, including the mobility emulation procedure, and presents the results. Section V concludes the paper.

II. SYSTEM MODEL

In this section, we describe the system design for the communication system and Doppler estimation and compensation method used in this work.

A. ZP-OFDM Scheme

The packet structure is shown in Fig. 2. It consists of a Doppler-resistant preamble and postamble pair that encapsulate the packet. To improve packet detection and synchronization under high-Doppler conditions, an additional preamble sequence consisting of a pseudorandom noise (PN) sequence precedes the zero-padded orthogonal frequency division multiplexing (ZP-OFDM) symbols. Each block in this packet structure is separated by guard intervals to counter interference due to multipath. The outer preamble and postamble pair are implemented with a single linear frequency modulated (LFM) pulse. This type of pulse retains its autocorrelation properties under the presence of Doppler shifts and, therefore, can be used to detect a packet in such conditions reliably. The postamble is used for Doppler scale estimation. Using the same pulse

for the preamble and postamble requires additional effort, such as incorporating timing information about packet structure for packet detection. Therefore, to differentiate the beginning and the end of the packet, the preamble and postamble sequences are implemented with up-chirp ($f_1 > f_0$), and down-chirp ($f_0 > f_1$), respectively. The PN preamble is implemented with a maximum length sequence and produces a distinct peak after correlation at the receiver, thanks to its autocorrelation properties. The matched filter output of the PN preamble produces better timing precision compared to the LFM preamble, thus it is the preferred method for timing synchronization for OFDM symbol demodulation. However, the correlation performance of the PN preamble deteriorates significantly if the Doppler effect is present, which limits its usefulness for packet detection and synchronization. Therefore, the two-preamble structure is implemented to ensure reliable packet detection and synchronization under all Doppler conditions.
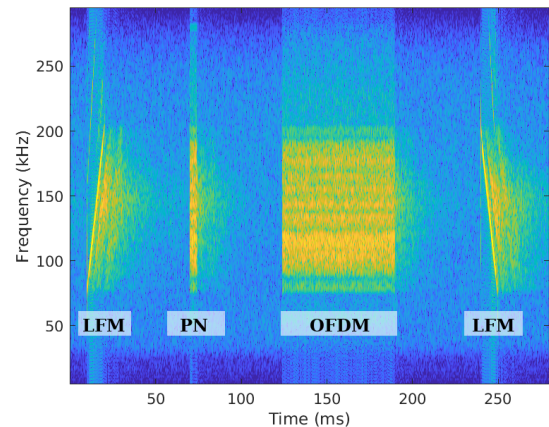

Fig. 2: Sections of a ZP-OFDM packet annotated on the spectrogram of a received packet

The OFDM symbol consists of differentially coherent BPSK encoded symbols such that the information bits are encoded in the phase difference between adjacent subcarriers [9]. This method does not utilize pilot based channel estimation method and therefore pilot subcarriers are not needed. Therefore, less complex receiver architectures can be used compared to coherent OFDM systems. For channel frequency offset estimation which will be described in the next section, null subcarriers are required. These subcarriers are not loaded with symbols and they are placed at equal intervals among data subcarriers. In this paper, 8192 subcarriers over 125 kHz bandwidth are used which results in a subcarrier bandwidth of 15.26 Hz. Two adjacent null subcarriers are placed at every 512 subcarriers, and the remaining 8144 are data subcarriers.

Due to high bandwidth, inevitably, some subcarriers will be received with errors because of fading under realistic operating conditions. Therefore, a forward error correction (FEC) system based on parallel concatenated convolutional codes, commonly known as turbo codes are implemented. The coding rate of the FEC is 1/3 and it provides better performance against bursts of errors that occur in adjacent subcarriers than convolutional

codes.

### B. Doppler Estimation and Compensation

Doppler shifts are constantly changing due to the environment and platform motion. Therefore, an accurate estimation of the Doppler scale factor and CFO for each packet is required for compensation. In this section, the two-step estimation and compensation procedure will be described.

The non-uniform Doppler effect causes compression or dilation of the packet, and Doppler scale estimation is performed by measuring the received packet duration as described in [6]. To estimate the duration, Doppler-resistant preamble and postamble sequences described in the packet structure section are used. Once a packet duration estimate is obtained, the packet is extrapolated with the linear interpolation method from available samples. This operation not only adds or removes samples to counter compression or dilation but also changes the values of the existing samples as if they were sampled at slightly different sample rates. The length of the resulting vector has the exact number of samples for packet duration such that the Doppler scale factor would be precisely "0". After non-uniform Doppler shifts are estimated and compensated, the preamble and postamble sections are removed from the packet, and synchronization is performed on the remaining using the cross-correlation method on the PN sequence. OFDM blocks are extracted for uniform Doppler estimation and the compensation procedure is applied to them as described in [3].

In the received packet, subcarriers are shifted in the frequency domain which causes misalignment. For estimation, the resulting leakage from adjacent subcarriers to null subcarriers is used as the metric. The energy on each null subcarrier is calculated and accumulated to find the total leakage. Then a nonlinear programming problem is formulated, which minimizes this metric by applying a variable frequency shift. The problem is further constrained such that the magnitude of the frequency shift is less than the subcarrier bandwidth and solved with *'fminbnd'* function. Note that, unlike other sections of the algorithm, the estimation procedure described here has varying convergence times. This can be an issue in real-time receiver systems with latency constraints. In such cases, optimizer parameters such as minimum step size and the maximum number of iterations should be adjusted to confine the execution time. Finally, OFDM blocks are compensated by applying the frequency shift estimated by the solver.

III. Experimental Setup

Performance evaluation of the Doppler compensation system is performed with experiments at the East Boston Marina. In these experiments, communication with ZP-OFDM packets is performed with platform mobility. Transmitted and recorded files were processed at the sampling rate of 2.5 Msps. The files are in baseband and upconversion and downconversion is performed at the digital signal processing (DSP) section of the modems. The files are stored on the main modems and processed offline on a host computer using MATLAB. For
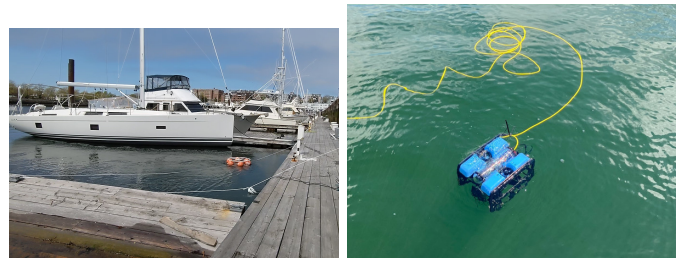
(a) Fixed trajectory   (b) Random trajectory

Fig. 3: Experimental setups for mobility emulation

these experiments, a 140 kHz center frequency is used as can be seen in Fig. 2.

A notable challenge when mobility is present is setting and recording the exact trajectory of the motion. A controllable environment is crucial to develop and testing the Doppler estimation and compensation performance, because external sources of disturbance such as waves, wind, and currents may have a significant impact on the trajectory. On the other hand, the algorithms need to work with actual motion profiles for underwater vehicles in realistic settings. To address these practical experimental issues, two settings are designed. In the first set of experiments, a mechanical system controlled by an operator is used. The second experimental setting instead uses an underwater vehicle as the mobile platform.

The fixed trajectory mobility setup is shown in 3a. The transmitter node is mounted on a buoy assembly rigidly, such that the node and the assembly move together. The receiver node is anchored to the dock approximately 1 meter below the surface. In this setup, platform motion is created by floating the transmitter node at the surface. Furthermore, to ensure a repeatable movement pattern a pulley system is set up on the dock. A rope is tied to two opposite sides of the buoy assembly and fed through two pulleys that are fixed to the two sides of the dock. This setup provides a repeatable movement pattern for two reasons. The trajectory is constrained on a straight line between two pulleys which limits influence from waves, wind, and operator positioning. The speed profile of the platform can be controlled with better accuracy since pulleys establish a low friction system and the two-rope setup allows rapid deceleration. A timer is used to adjust the pace.

An important design factor of the non-uniform Doppler estimation performance is the parameter set of the preamble sequence. As noted in Section II-A Doppler resistant preamble sequences are used for packet duration estimation. The bandwidth and the duration of the LFM preambles along with packet duration detection sensitivity and estimation resolution [6].

In order to investigate the effect of these parameters, a test set given in Table I is generated. The rest of the packet parameters are kept the same. To be able to compare these against each other, they need to experience the same relative motion and therefore, the fixed trajectory mobility setup is used to generate repeatable movement patterns, as explained previously.

TABLE I
PREAMBLE PARAMETERS

Preamble Type	Preamble Duration [ms]	Packet Duration [ms]
LFM	2	224
LFM	5	240
LFM	10	250
LFM	20	270
QFM	10	250

In the random trajectory setup, the receiver node is anchored to the dock 1 meter deep, similar to the fixed trajectory setup, and a remotely operated vehicle (ROV) is used as the mobile platform for the transmitter node. The transmitter integrated to a BlueROV2 as described in [10] and the node is shown in Fig. 3b. In this configuration, the modem is mounted under the ROV with the transducer element facing forward. At this location, the visibility was limited due to the turbidity of the water, which not only makes it difficult to see the position of the mobile platform from the dock but also reduces visual cues from the ROV video feed. Therefore the compass bearing and the depth information supplied by onboard sensors of the ROV are used as the main navigational aid for setting the course, and steering adjustments were made based on the video input. Long horizontal trajectories near the surface were impractical due to ongoing marine traffic and strong currents. Therefore, the region directly below the receiver node is preferred, and a high acceleration profile is used.

IV. EXPERIMENTAL RESULTS

We start our analysis by first evaluating subcarrier-level performance, and then we will focus on packet-level performance.

A predominant symptom of the Doppler effect is the distortion and scattering of the symbols. In Fig. 4, constellation diagrams before and after Doppler compensation are shown for a BPSK-modulated ZP-OFDM packet from the fixed trajectory mobility scenario. It can be seen that the decision regions of the compensated system can easily be separated, unlike the uncompensated system in which the symbols are scattered more.
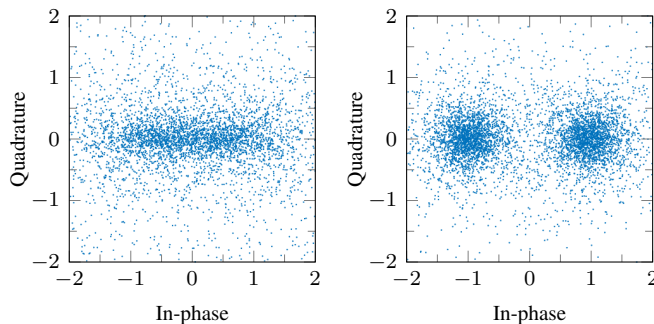

Fig. 4: Constellation of received signal before and after uniform and non-uniform Doppler compensation

The effect of platform motion can also be observed through subcarrier energy levels. Mean subcarrier energy levels before

and after Doppler compensation is illustrated in Fig. 5. In the figure, received energy levels in frequency bins are calculated for 94 packets from the same recording used previously, and these levels are averaged. For better visualization, a small subset of contiguous subcarriers the total OFDM bandwidth (1.68 kHz of 125 kHz) is shown in these figures. Measured subcarrier energy levels throughout this region of frequencies are expected to be relatively flat except for null subcarriers. The measurements are applicable to other parts of the spectrum though frequency-dependent attenuation is present. Compensated and uncompensated packets have the same total energy, but there are significant differences in how the energy is distributed into subcarriers. The variance of energy levels of data subcarriers after Doppler compensation is lower than that of an uncompensated packet. In addition, two null subcarriers at indices 511 and 512 have substantial leakage before Doppler compensation.
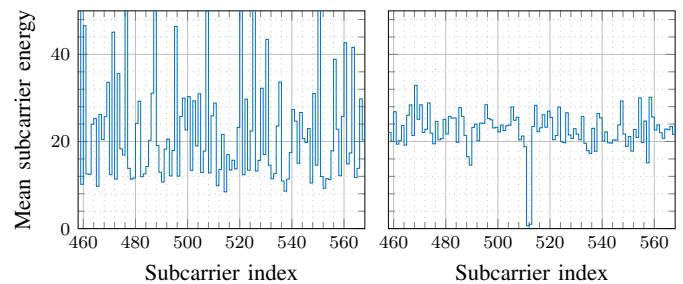

Fig. 5: Estimated mean energy levels of individual subcarriers before and after Doppler compensation

The subcarrier interference discussed here should not be considered the definitive indicator for the Doppler effect since system design parameter selection and channel effects can lead to similar distortion effects. Furthermore, even though not shown here, signal-to-noise ratios for the uncompensated and compensated systems are the same as explained in the mean subcarrier energy level discussion and therefore the SNR metric is also not indicative for diagnosing this effect. These metrics are not effective on their own. As discussed in the next part, the packets cannot be received at the desired performance level for further diagnosis, which poses a challenge when developing the physical layer of a communication system. Therefore it is crucial to embed a Doppler estimation method into the receiver to detect Doppler-induced distortion in high-frequency, high-bandwidth underwater acoustic systems.

The fixed trajectory is planned as follows. Initially, the transmitter modem is at the farthest position from the receiver, then it moves to the mid-point in 6 seconds and stops, then moves next to the receiver modem in 6 seconds. From this point, it returns to its initial position in about 8 seconds. Each part of the movement has around 2 seconds of wait time in between, including the very beginning and end of the recording. The total duration of the recording is approximately 28 seconds. The calculated bit error rates per packet and estimated relative speed of the transmitter node for the fixed

trajectory mobility scenario are given in Figs. 6 and 7. The relative speed is estimated from the received signal using the method described in Sec. II-B. In Fig. 6, bit error rates are given for packets at various stages of the processing to emphasize the contribution of each step of the receiver processing. The four traces correspond to bit error rates of uncompensated, non-uniform compensation, combined non-uniform and uniform Doppler compensation, and forward error correction after compensation. To calculate bit error rates with and without forward error correction, data symbols that correspond to encoded bits of the payload are stored in addition to the payload. The encoded bits are used to calculate bit error rates before channel decoding.
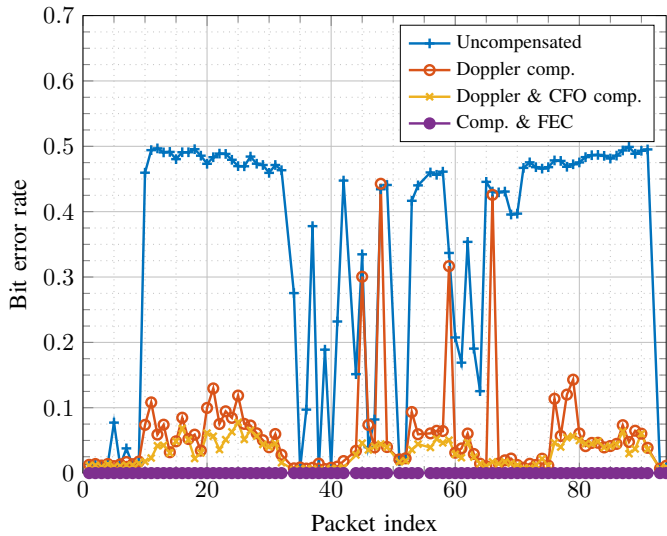

Fig. 6: Bit error rates per packet for fixed trajectory mobility scenario
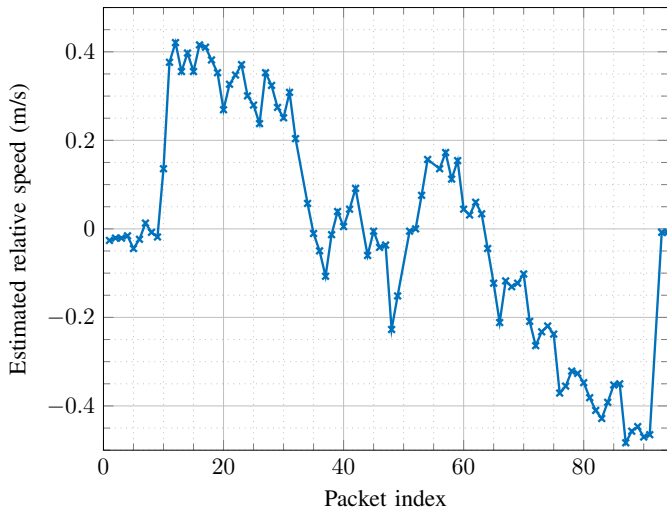

Fig. 7: Estimated relative speed of the system for fixed trajectory mobility scenario

These results indicate a strong correlation between the BER

and the relative speed. When platform motion is present, the BER in the uncompensated system increases to 0.5, and payload data cannot be recovered in this case. It can be seen that the non-uniform and uniform Doppler compensation gradually reduces BER and the bulk of the improvement is due to the non-uniform part. After FEC, no bit errors are present and each packet was recovered error-free. Note that the FEC can provide resiliency against this type of distortion without any compensation. The maximum BER it can correct in this way was 9×10^{-2}, which is observed at a Doppler scale factor of 3.3×10^{-5}.

For the random trajectory mobility scenario, the ROV platform is initially submerged with some horizontal offset such that a direct path exists between transmitter and receiver transducers. Then the platform is moved up and down by the operator as the depth information is the most precise input. Unlike the fixed trajectory mobility setup, the exact trajectory is not known due to lack of precise localization information, instead, the relative speed is extracted from the recording. The calculated bit error rates per packet and estimated speed of the mobile node are given in Figs. 8 and 9. For brevity, bit error rates are shown only for the uncompensated and fully compensated system with forward error correction.
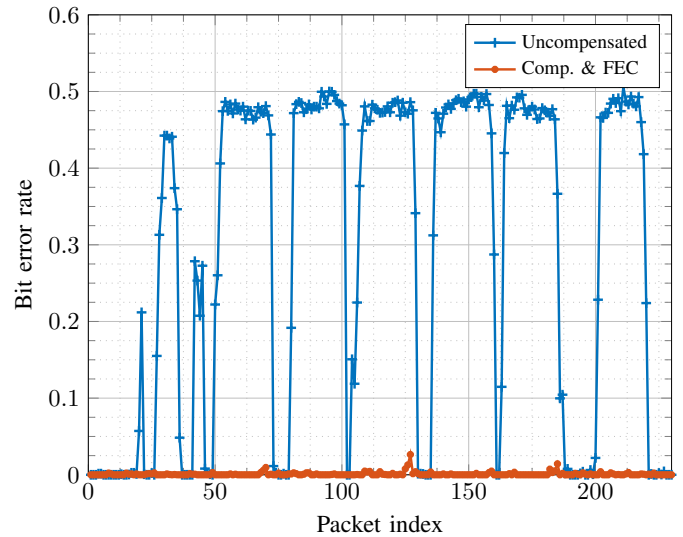

Fig. 8: Bit error rates per packet for random trajectory mobility scenario

The BER results of the random trajectory mobility scenario exhibit a similar correlation trend to the fixed trajectory scenario. In this recording, however, the FEC was unable to correct all of the packets and the BER for the recording is calculated as 9.1×10^{-4}. Packets with the most number of bit errors are received at the time instances in which the direction of the relative movement changes. Furthermore, the channel response can vary significantly in this scenario since the initial direct path setup is not guaranteed to be preserved due to unintended horizontal motion.

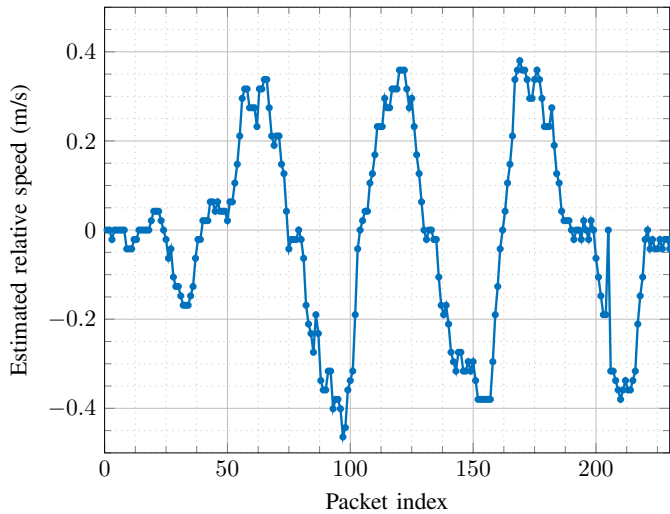Finally, using the fixed trajectory mobility scenario, differ-

Fig. 9: Estimated relative speed of the mobile platform for random trajectory mobility scenario
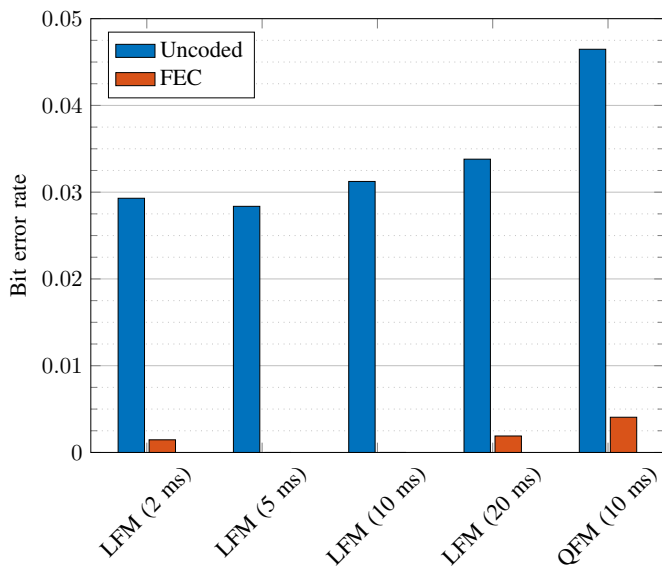

Fig. 10: Average bit error rates for different preamble types in fixed trajectory mobility

ent preamble configurations listed in Table I for Doppler scale factor estimation are evaluated. Bit error rates calculated from these recordings are given in Fig. 10.

In this figure, the BER performance of Doppler compensated packets is shown without and with FEC similar to the third and fourth traces of Fig. 6. It can be seen that the variance between these preamble configurations is not significant and in most cases, FEC can successfully eliminate all of the errors. Note that even though the mobility emulation setup allows repeatable mobility experiments, the actual speed profile will differ due to the operator, and the BER performance is influenced by other factors such as interference during the

experiments. Therefore, these levels indicate that the preamble configurations work well for this setup.

V. CONCLUSIONS

In this work, we presented a set of field experiments with a multicarrier communication system incorporating a Doppler estimation and compensation method. Large-bandwidth underwater acoustic communication systems operating on high carrier frequencies are highly sensitive to motion-induced Doppler effect which can result in severe distortion due to inter-carrier interference even at relatively slow speeds. The design of ZP-OFDM packet structure and the Doppler estimation and compensation procedure is described as well as mobility emulation setups that are used to generate fixed trajectories and random trajectories.

Field experiments were performed with software-defined underwater acoustic modems and an ROV platform. For each trajectory, the efficacy of the two-step compensation process is investigated. It is shown that the system can provide error-free communication under the presence of platform motion-induced Doppler effect in most cases with the help of forward error correction.

REFERENCES

[1] M. Stojanovic and J. Preisig, "Underwater acoustic communication channels: Propagation models and statistical characterization," *IEEE Communications Magazine*, vol. 47, no. 1, pp. 84–89, January 2009.

[2] T. Melodia, H. Kulhandjian, L. Kuo, and E. Demirors, "Advances in underwater acoustic networking," in *Mobile Ad Hoc Networking: Cutting Edge Directions*, 2nd ed., S. Basagni, M. Conti, S. Giordano, and I. Stojmenovic, Eds. Inc., Hoboken, NJ: John Wiley and Sons, 2013, pp. 804–852.

[3] B. Li, S. Zhou, M. Stojanovic, L. Freitag, and P. Willett, "Multicarrier communication over underwater acoustic channels with nonuniform doppler shifts," *IEEE Journal of Oceanic Engineering*, vol. 33, no. 2, pp. 198–209, April 2008.

[4] A. Radosevic, R. Ahmed, T. M. Duman, J. G. Proakis, and M. Stojanovic, "Adaptive ofdm modulation for underwater acoustic communications: Design considerations and experimental results," *IEEE Journal of Oceanic Engineering*, vol. 39, no. 2, pp. 357–370, 2014.

[5] M. Stojanovic, J. Catipovic, and J. Proakis, "Phase Coherent Digital Communications for Underwater Acoustic Channels," *IEEE Journal of Oceanic Engineering*, vol. 19, no. 1, pp. 100–111, Jan. 1994.

[6] B. Sharif, J. Neasham, O. Hinton, and A. Adams, "A computationally efficient doppler compensation system for underwater acoustic communications," *IEEE Journal of Oceanic Engineering*, vol. 25, no. 1, pp. 52–61, January 2000.

[7] K. A. Perrine, K. F. Nieman, T. L. Henderson, K. H. Lent, T. J. Brudner, and B. L. Evans, "Doppler estimation and correction for shallow underwater acoustic communications," in *2010 Conference Record of the Forty Fourth Asilomar Conference on Signals, Systems and Computers*, 2010, pp. 746–750.

[8] F. Qu, Z. Wang, L. Yang, and Z. Wu, "A journey toward modeling and resolving doppler in underwater acoustic communications," *IEEE Communications Magazine*, vol. 54, no. 2, pp. 49–55, 2016.

[9] A. Tadayon and M. Stojanovic, "Low-complexity superresolution frequency offset estimation for high data rate acoustic ofdm systems," *IEEE Journal of Oceanic Engineering*, vol. 44, no. 4, pp. 932–942, 2019.

[10] D. Unal, S. Falleni, E. Demirors, K. Enhos, S. Basagni, and T. Melodia, "A software-defined underwater acoustic networking platform for underwater vehicles," in *ICC 2022 - IEEE International Conference on Communications*, 2022, pp. 2531–2536.